



# Non-isothermal preform infiltration during the vacuum-assisted resin transfer molding (VARTM) process

M. Grujicic<sup>a,\*</sup>, K.M. Chittajallu<sup>a</sup>, Shawn Walsh<sup>b</sup>

<sup>a</sup>Department of Mechanical Engineering, Clemson University, 241 Fluor Daniel, Clemson, SC 29634-0921, USA

<sup>b</sup>Army Research Laboratory–WMRD AMSRL-WM-MD, Aberdeen, Proving Ground, MD 21005-5069, USA

Received 7 March 2004; received in revised form 23 September 2004; accepted 23 September 2004

Available online 2 December 2004

## Abstract

A control-volume finite-element model is developed to analyze the infiltration of a fiber preform with resin under non-isothermal conditions within a high-permeability resin-distribution medium based vacuum-assisted resin transfer molding (VARTM) process. Due to the exposure to high temperatures during preform infiltration, the resin first undergoes thermal-thinning which decreases its viscosity. Subsequently however, the resin begins to gel and its viscosity increases as the degree of polymerization increases. Therefore, the analysis of preform infiltration with the resin entails the simultaneous solution of a continuity equation, an energy conservation equation and an evolution equation for the degree of polymerization. The model is applied to simulate the infiltration of a rectangular carbon fiber based preform with the NBV-800 epoxy resin and to optimize the VARTM process with respect to minimizing the preform infiltration time. The results obtained suggest that by proper selection of the ramp/hold thermal history of the tool plate, one can reduce the preform infiltration time relative to the room-temperature infiltration time. This infiltration time reduction is the result of the thermal-thinning induced decrease in viscosity of the ungelled resin.

© 2004 Elsevier B.V. All rights reserved.

PACS: 61.41.+e (Polymers)

Keywords: Vacuum-assisted resin transfer molding (VARTM) process; Modeling and simulations

## 1. Introduction

Vacuum-assisted resin transfer molding (VARTM) is an open-mold polymer-matrix composite manu-

facturing process widely used in a variety of commercial applications (e.g. boats, refrigerated cargo boxes, etc.). In addition, the VARTM process is being considered for different automotive, aerospace and military applications [1–3]. The process is based on the use of a single rigid mold (tool plate) which is laid up with fiber-reinforcement preforms and enclosed in an air-impervious vacuum bag. The

\* Corresponding author. Tel.: +1 864 656 5639;

fax: +1 864 656 4435.

E-mail address: [mica.grujicic@ces.clemson.edu](mailto:mica.grujicic@ces.clemson.edu) (M. Grujicic).

# Report Documentation Page

Form Approved  
OMB No. 0704-0188

Public reporting burden for the collection of information is estimated to average 1 hour per response, including the time for reviewing instructions, searching existing data sources, gathering and maintaining the data needed, and completing and reviewing the collection of information. Send comments regarding this burden estimate or any other aspect of this collection of information, including suggestions for reducing this burden, to Washington Headquarters Services, Directorate for Information Operations and Reports, 1215 Jefferson Davis Highway, Suite 1204, Arlington VA 22202-4302. Respondents should be aware that notwithstanding any other provision of law, no person shall be subject to a penalty for failing to comply with a collection of information if it does not display a currently valid OMB control number.

1. REPORT DATE <b>2005</b>		2. REPORT TYPE		3. DATES COVERED <b>00-00-2005 to 00-00-2005</b>	
4. TITLE AND SUBTITLE <b>Non-isothermal preform infiltration during the vacuum-assisted resin transfer molding (VARTM) process</b>				5a. CONTRACT NUMBER	
				5b. GRANT NUMBER	
				5c. PROGRAM ELEMENT NUMBER	
6. AUTHOR(S)				5d. PROJECT NUMBER	
				5e. TASK NUMBER	
				5f. WORK UNIT NUMBER	
7. PERFORMING ORGANIZATION NAME(S) AND ADDRESS(ES) <b>Celmsn University, Department of Mechanical Engineering, Clemson, SC, 29634</b>				8. PERFORMING ORGANIZATION REPORT NUMBER	
9. SPONSORING/MONITORING AGENCY NAME(S) AND ADDRESS(ES)				10. SPONSOR/MONITOR'S ACRONYM(S)	
				11. SPONSOR/MONITOR'S REPORT NUMBER(S)	
12. DISTRIBUTION/AVAILABILITY STATEMENT <b>Approved for public release; distribution unlimited</b>					
13. SUPPLEMENTARY NOTES					
14. ABSTRACT <b>A control-volume finite-element model is developed to analyze the infiltration of a fiber preform with resin under nonisothermal conditions within a high-permeability resin-distribution medium based vacuum-assisted resin transfer molding (VARTM) process. Due to the exposure to high temperatures during preform infiltration, the resin first undergoes thermal thinning which decreases its viscosity. Subsequently however, the resin begins to gel and its viscosity increases as the degree of polymerization increases. Therefore, the analysis of preform infiltration with the resin entails the simultaneous solution of a continuity equation, an energy conservation equation and an evolution equation for the degree of polymerization. The model is applied to simulate the infiltration of a rectangular carbon fiber based preform with the NBV-800 epoxy resin and to optimize the VARTM process with respect to minimizing the preform infiltration time. The results obtained suggest that by proper selection of the ramp/hold thermal history of the tool plate, one can reduce the preform infiltration time relative to the room-temperature infiltration time. This infiltration time reduction is the result of the thermal-thinning induced decrease in viscosity of the ungelled resin.</b>					
15. SUBJECT TERMS					
16. SECURITY CLASSIFICATION OF:			17. LIMITATION OF ABSTRACT <b>Same as Report (SAR)</b>	18. NUMBER OF PAGES <b>14</b>	19a. NAME OF RESPONSIBLE PERSON
a. REPORT <b>unclassified</b>	b. ABSTRACT <b>unclassified</b>	c. THIS PAGE <b>unclassified</b>			

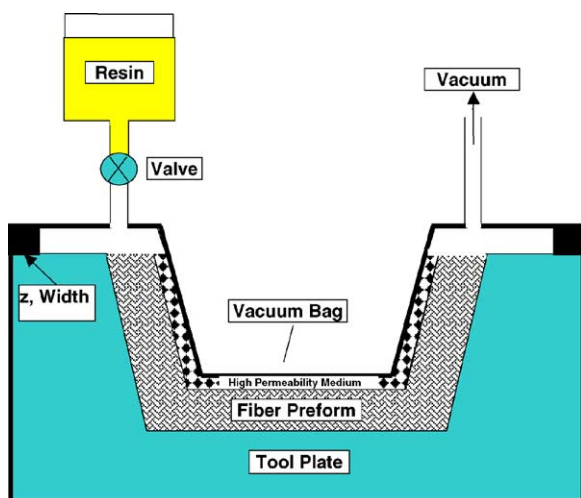


Fig. 1. Schematic of the vacuum-assisted resin transfer molding (VARTM) process.

preform is next infiltrated with resin using vacuum pressure, Fig. 1. Lastly, the rigid mold is heated to a resin-dependent temperature and held at that temperature for a sufficient amount of time to ensure a complete curing of the resin-impregnated preform. The VARTM process offers several advantages over the competing polymer-matrix composites manufacturing processes such as: (a) a low tooling cost; (b) a low emission of volatile organic chemicals; (c) processing flexibility; (d) a low void-content in the fabricated parts; and (e) a potential for fabrication of the relatively large (surface area  $\sim 150\text{--}200\text{ m}^2$ ) and thick (0.1–0.15 m) composite parts, containing a large content (75–80 wt.%) of the reinforcing fiber-preform phase.

There are several versions of the VARTM process which differ mainly with respect to the type of resin distribution system used. Among these, two are most frequently used: (a) a VARTM process based on the use of a high-permeability medium, Fig. 2(a); and (b) a VARTM process based on the use of grooves located within a low-density core of the fiber preform, Fig. 2(b).

While the VARTM process has been commercialized for more than a decade, its application to manufacture of complex composite structures is based almost entirely on experience and on a trial-and-error approach. One of the most critical steps during the VARTM process is the resin infiltration stage. Ideally,

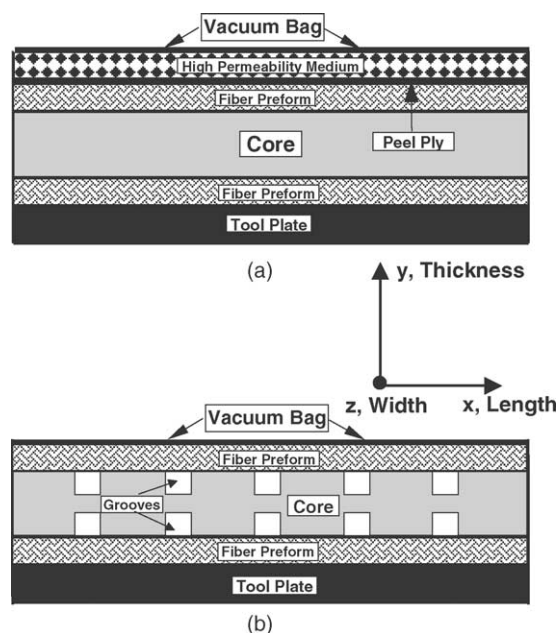


Fig. 2. Two common types of resin distribution systems used in VARTM. (a) A high-permeability medium based system; and (b) a grooves based system.

one would want a complete infiltration of the preform (mold filling) with the resin, in a shortest period of time in order to minimize the production time and, thus, the manufacturing cost. In addition, one must ensure that the resin completely wets the fiber preform in order to avoid formation of “dry spots”. Due to a lack of polymer–fiber bonding, dry spots can act as crack nucleation sites, when VARTM-fabricated structures are subjected to loads while in service. In general, polymerization (gelation) of the resin should not take place during the mold-filling stage, since the resulting increase in resin viscosity may lead to incomplete preform infiltration. Therefore, computer models which can provide a better understanding of the fiber-preform infiltration process and enable an accurate prediction of the infiltration time, should help the manufacturers of composite structures to design and optimize the VARTM process so that, through the selection of the tool-plate heating profile and the resin composition (e.g. the concentrations of infiltration solvent, initiator, etc.), a complete mold filling is attained in a shortest period of time. In a series of papers, Lee and co-workers [4–8] developed a finite-element control-volume based model for isothermal,

preform filling for both high-permeability medium and grooves-based VARTM processes. The models developed by Lee and co-workers [4–8] enable the prediction of the filling time and the flow pattern and were validated by comparing the model predictions with the (room-temperature) flow-visualization experimental results for preform infiltration with several oils of different viscosity. In a typical VARTM process, heating of the tool-plate is started only after the mold-filling stage of the process is completed. Under such conditions, the models developed by Lee and co-workers [4–8] can be used to analyze the mold filling process. However, one may identify at least two potential benefits that heating of the tool plate during the resin infiltration stage of the VARTM process can have: (a) moisture absorbed onto the fiber-preform surface could be removed to a greater extent promoting a better-polymer/fiber bonding; and (b) temperature-induced lowering of the viscosity of the “ungelled” resin can facilitate a more complete mold filling and give rise to shorter infiltration times. Due to the isothermal nature of the models developed by Lee and co-workers [4–8], they cannot be used to analyze the preform infiltration process under the conditions when the tool plate is being heated and a non-uniform, time-dependent temperature field is developed in the mold. To overcome these limitations, the (isothermal) two-dimensional finite-element control-volume mold-filling model of Lee and co-workers [4] for the VARTM process based on the use of a high-permeability medium, is extended to account for the thermal effects and the associated changes in the degree of polymerization and in turn, in the resin viscosity.

The organization of the paper is as follows. In Sections 2.1–2.3, brief descriptions are given of the governing equations, the finite-element control-volume method and its two-dimensional implementation, respectively. Temperature and time effects on the degree of polymerization and in turn, on the viscosity of the NBV-800, a two-component, toughened, 400 K-curing, epoxy-type VARTM resin [9], are discussed in Section 3. The main flow-front mold-filling and the filling-time results obtained in the present work are presented and discussed in Section 4, while the key conclusions resulting from the present work are summarized in Section 5.

## 2. Computational procedure

### 2.1. Formulation of the model

#### 2.1.1. General consideration

The mold-filling model developed in the present work is based on the following assumptions and simplifications:

- (a) fiber preform placed into the mold cavity prior to its infiltration with resin does not undergo any rigid-body motion during mold filling but can undergo reversible deformations due to a pressure difference across the vacuum-bag walls which affects preform permeability;
- (b) due to a low value of the Reynolds number of the resin flow, inertia effects are negligible;
- (c) the effects of surface tension are negligible in comparison with the viscous-force effects;
- (d) the size of the mold cavity is much larger than the average fiber-preform pore size so that the momentum conservation equation can be replaced by the Darcy’s law for fluid flow through a porous medium; and
- (e) the resin can be considered as an incompressible fluid.

The steady-state resin flow is governed by the following incompressible-fluid continuity equation:

$$\nabla \cdot \vartheta = 0 \quad (1)$$

where  $\nabla \cdot$  denotes a divergence operator, and  $\vartheta$  the resin velocity vector.

Integration of Eq. (1) over a control-volume,  $V_{CV}$ , gives:

$$\int_{V_{CV}} \nabla \cdot \vartheta \, dV = 0 \quad (2)$$

where  $V$  denotes the volume and, through the use of the divergence theorem, Eq. (2) can be transformed into:

$$\int_{S_{CV}} \vartheta \cdot n \, dS = 0 \quad (3)$$

where  $S$  denotes the surface,  $S_{CV}$  the surface of a control-volume,  $n$  the outward unit vector normal to the surface of the control-volume and the raised

dot is used to represent a scalar product of two vectors.

The Darcy's law for flow through a porous medium can be expressed as:

$$\vartheta = -\frac{K}{\mu} \nabla P \quad (4)$$

where  $K$  is a second-order permeability tensor,  $\mu$  resin viscosity and  $\nabla$  denotes a gradient operator.

Substitution of Eq. (4) into (3) yields:

$$\int_{S_{cv}} \frac{1}{\mu} n K \nabla P \, dS = 0 \quad (5)$$

While Eq. (5) is derived starting from the steady-state continuity Eq. (1), it is used in the present study to analyze the transient fluid flow during mold filling. This is justified by the fact that mold filling takes place at a relatively low rate and can be considered as a quasi steady-state process in which a steady-state condition can be assumed to hold over each small time step.

The control-volume formulation developed up to this point is applicable only for an isothermal mold-filling process. To include the effect of temperature, in addition to the continuity equation, Eq. (1), one must also consider the energy conservation equation. Since, in general, carbon-based fiber preforms have good thermal conductivity, thermal conduction is expected to be an important mechanism for transfer of the heat from the tool-plate, through the fiber preform to the resin. In addition, the transfer of heat by the moving resin is also expected to play a significant role. To simplify the resulting energy conservation equation, a homogenization approach is used which eliminates a separate treatment of the fiber preform and resin in a control-volume and, instead, uses effective (volume-averaged) gravimetric and thermal properties of the materials in a control-volume. Under such conditions, the energy conservation equation is defined as:

$$\rho C_p \frac{\partial T}{\partial t} + \rho C_p \vartheta \cdot \nabla T + \nabla \cdot (-k \nabla T) = Q_s \quad (6)$$

where  $\rho$ ,  $C_p$  and  $k$  denote the effective density, heat capacity and thermal conductivity, respectively,  $T$  the temperature, and  $Q_s$  a heat sink or a heat source term.

### 2.1.2. Two-dimensional formulation

In the following analysis, preform length is assumed to be aligned in the  $x$ -direction, preform thickness in the  $y$ -direction and preform width in the  $z$ -direction. In many VARTM applications, the width of the fiber preform does not vary along the length of the preform and, hence, the mold geometry and its filling can be simplified using a two-dimensional representation. When the preform is curved along its length, a local coordinate system is used whose  $z$ -axis is still aligned in the preform width direction. Constant pressure is assumed to exist in the  $z$ -direction and hence, the pressure is assumed to be only a function of the local  $x$  and  $y$  coordinates. However, since resin viscosity (due to gradients of the degree of polymerization and temperature in the width direction) and differences in the preform permeability may vary in the width direction, a width averaged resin velocity is defined, within a three-dimensional Cartesian coordinate system, as:

$$\bar{\vartheta}(x, y) = \frac{1}{w_z} \int_0^{h_z} \vartheta(x, y, z) \, dz \quad (7)$$

where  $w_z$  is the local preform width and an overbar is used to denote an average quantity. Substitution of Eq. (7) into Eq. (5) yields a two-dimensional case:

$$\begin{aligned} & \int_{C_{cv}} w_z n S \nabla P \, dl \\ &= \int_{C_{cv}} w_z [n_x \quad n_y] \begin{bmatrix} S_{xx} & S_{xy} \\ S_{yx} & S_{yy} \end{bmatrix} \begin{bmatrix} \frac{\partial P}{\partial x} \\ \frac{\partial P}{\partial y} \end{bmatrix} dl = 0 \end{aligned} \quad (8)$$

where

$$S = \frac{1}{w_z} \int_0^{h_z} \frac{K'}{\mu} \, dz \quad (9)$$

is a  $2 \times 2$  flow-coefficient matrix defined in terms of the width-averaged resin viscosity and the width-averaged preform permeability matrix,  $K'$ . Assuming that the preform width is uniformed over the surface area of a single control-volume, the surface integral in Eq. (8) is replaced by a product of the preform width at the location of a given control-volume and the corresponding line integral.

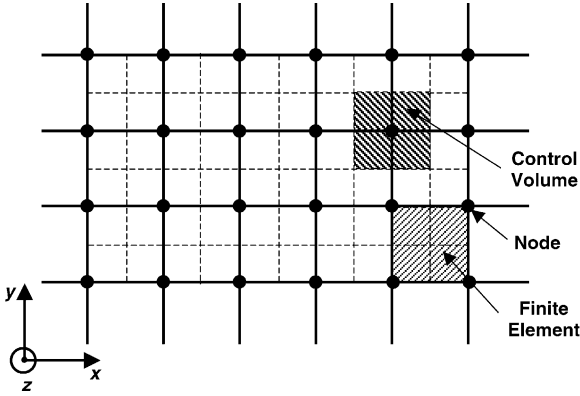


Fig. 3. Discretization of the computational domain into four-node quadrilateral finite-elements and quadrilateral control-volumes.

2.2. Finite-element implementation

In this section, Eq. (8) and a finite-element control-volume method are used to develop a model for simulation of a two-dimensional mold filling process. Toward that end, the entire flow field is divided into four-node quadrilateral elements, as schematically shown in Fig. 3. Next centroids of the four adjacent elements are connected with straight lines to form quadrilateral control-volumes (more precisely control areas in the present two-dimensional formulation). As shown in Fig. 4, each control area is composed of four

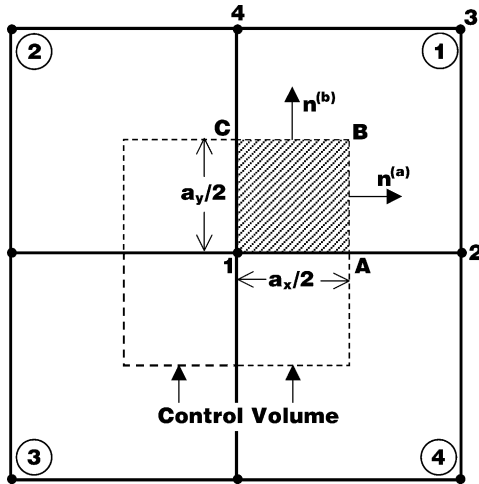


Fig. 4. Control-volume is composed of four quadrilateral segments each residing in a different finite-element (encircled number). Outward control-volume surface normals are denoted by  $n$ .

sub-regions each associated with a different finite-element (element numbers are encircled in Fig. 4).

Next, following the standard finite-element formulation, the pressure at each point within an element is defined in terms of the pressures at the four nodes,  $P_i$  ( $i = 1-4$ ), as;

$$P = \sum_{i=1}^4 P_i N_i \tag{10}$$

where the four bi-linear shape functions,  $N_i$  ( $i = 1-4$ ), are defined in terms of a control-volume based  $x' - y'$  coordinate system whose origin is located at the lower-left node of the element as:

$$\begin{aligned} N_1 &= \frac{(a_x - x')(a_y - y')}{A}, & N_2 &= \frac{x'(a_y - y')}{A}, \\ N_3 &= \frac{x'y'}{A}, & N_4 &= \frac{(a_x - x')y'}{A} \end{aligned} \tag{11}$$

where  $a_x$  and  $a_y$  are the width and the height of an element respectively, and the element surface area  $A \equiv a_x a_y$ .

Partial derivatives of the shape functions  $\alpha_i \equiv dN_i/dx'$  and  $\beta_i \equiv dN_i/dy'$  are then computed as:

$$\begin{aligned} \alpha_1(y') &= \frac{-(a_y - y')}{A}, & \alpha_2(y') &= \frac{(a_y - y')}{A}, \\ \alpha_3(y') &= \frac{y'}{A}, & \alpha_4(y') &= \frac{-y'}{A}, \\ \beta_1(x') &= \frac{-(a_x - x')}{A}, & \beta_2(x') &= \frac{-x'}{A}, \\ \beta_3(x') &= \frac{x'}{A}, & \beta_4(x') &= \frac{(a_x - x')}{A} \end{aligned} \tag{12}$$

Substitution of Eq. (12) into Eq. (8) yields:

$$\int_{C_{cv}} w_z n S B P dl = 0 \tag{13}$$

where

$$B = \begin{bmatrix} \alpha_1(y') & \alpha_2(y') & \alpha_3(y') & \alpha_4(y') \\ \beta_1(x') & \beta_2(x') & \beta_3(x') & \beta_4(x') \end{bmatrix} \tag{14}$$

and

$$P = [P_1 \ P_2 \ P_3 \ P_4]^T \tag{15}$$

and the superscript T is used to denote a transpose.

As seen in Fig. 4, the control-volume boundary within each element consists of two straight segments and, hence, the contour integral given in Eq. (13) can be rewritten as:

$$\sum_{i=1}^4 w_z \left[ \int_{C_{cv}} n_i^{(a)} S_i B_i^{(a)} P_i^{(a)} dl^{(a)} + \int_{C_{cv}} n_i^{(b)} S_i B_i^{(b)} P_i^{(b)} dl^{(b)} \right] = 0 \quad (16)$$

where superscripts (a) and (b) are used to denote the two line segments within a given element and subscript *i* to indicate the finite-elements associated with a given control-volume.

Upon integration, Eq. (16) for each control-volume becomes a linear algebraic equation of the pressures associated with the node coinciding with the centroid of the control-volume in question and with the surrounding eight nodes. After Eq. (16) is written for all control-volumes within the flow field and the appropriate boundary conditions for pressure are applied, a system of linear algebraic equations for the unknown pressures is obtained. The size of the system increases as the mold filling proceeds until the filling is complete.

The two-dimensional finite-element control-volume model presented thus far is strictly valid only for planar geometries in which the local coordinate system coincides with the global coordinate system. In addition, the *z*-axis is aligned with the preform width. However, for curved thin three-dimensional preforms, the local coordinate system whose orientation varies along the surface of the preform generally differs from the global coordinate system. In such cases, the local *z*-axis is still aligned with the preform width. However, before the current formulation can be applied, all the quantities of a control-volume defined with respect to the global coordinate system must be transformed into the local coordinate system. This procedure is briefly discussed in Appendix A.

The solution of the energy conservation equation, Eq. (6), is carried out using the same type of four-node quadrilateral finite-elements Eq. (10), and the same bilinear shape functions, Eq. (11). The solution to this problem can be found in many finite-element books (e.g. Eq. (8.13), P. 354 in Ref. [10]) and hence, is not repeated here.

It should be noted that since the temperature-dependent resin viscosity appears in the continuity equation, Eq. (5), and pressure-dependent resin velocities appear in the energy conservation equation, Eq. (6), the two equations are coupled. The procedure used to handle coupling of the two equations is described in the next section.

### 2.3. A two-dimensional mold filling model

The model developed in the previous section is used here to analyze two-dimensional mold filling. For simplicity, the preform is assumed to be rectangular in shape with its horizontal and vertical dimensions set to 0.1 m and 0.01 m, respectively. The thicknesses of the high-permeability medium, the peel ply and the fiber preform are set to 0.002 m, 0.0005 m, and 0.0075 m, respectively. The in-plane permeabilities for the high-permeability medium, the peel ply and the fiber preform in the absence of a pressure difference across the wall of the vacuum bag are assigned typical values of 2800 darcy (1 darcy =  $1.0 \times 10^{-12} \text{ m}^2$ ), 60 darcy and 60 darcy, respectively. The corresponding through-the-thickness permeabilities are also set to their typical values of 2800 darcy, 10 darcy and 10 darcy, respectively. To account for the effect of such pressure difference, the model and the model parameters proposed by Johnson and Pitchumani [11] are used. Viscosity of the resin and its variation with the degree of polymerization and temperature are described in next section. The remaining thermal properties of the fiber preform and the NBV-800 resin are listed in Table 1.

The computational domain is discretized into four-node quadrilateral elements of the size  $0.0005 \text{ m} \times 0.0005 \text{ m}$ . This yielded the following numbers of the finite-elements in the thickness direction in the high-permeability medium (4), peel ply (1) and the fiber preform (15).

Mold filling is carried out under the following boundary conditions:

- (1) Resin is allowed to enter the computational domain at the left-hand edge of the computational domain.
- (2) The pressure at the inlet is specified and set equal to the atmospheric pressure ( $P_{in} = 101,325.33 \text{ Pa}$ ).

Table 1  
Thermal properties of the carbon fiber preform and the NBV-800 epoxy resin

Property	Symbol	Unit	NBV-800 Resin	Carbon-fiber preform	High permeability medium	Peel ply
Density	$\rho$	kg/m <sup>3</sup>	$1.2 \times 10^3$	$2.0 \times 10^3$	$2.0 \times 10^3$	$2.0 \times 10^3$
Heat Capacity	$C_p$	J/kg/K	$0.7 \times 10^3$	$0.75 \times 10^3$	$0.6 \times 10^3$	$0.6 \times 10^3$
Thermal Conductivity	$k$	W/m/K	0.5	10	1.5	1.5
Volume Fraction	$f_v$	N/A	Balance	0.7	0.4	0.6
In-plane Permeability	$K$	Darcy	N/A	60	2800	60
Through-the-thickness Permeability	$K$	Darcy	N/A	102800	10	
Room-temperature Neat-resin Viscosity	$\eta$	cps	300	N/A	N/A	N/A
Room-temperature fully-cured resin viscosity	$\eta$	cps	10000	N/A	N/A	N/A

- (3) The pressure at the flow front is specified and set equal to the absolute vacuum pressure ( $P_{\text{vac}} = 0$  Pa).
- (4) A filled-fraction parameter ( $0 \leq f \leq 1$ ) is used to denote the volume fraction of the resin in a control-volume at the flow front.
- (5) The control-volumes associated with the inlet are assumed to be filled ( $f = 1$ ) at the onset of a mold-filling simulation run.
- (6) Pressure at the centroid of partially-filled ( $0 < f < 1$ ) control-volumes at the flow front are set to  $P_{\text{vac}}$ .
- (7) Since there is no resin flow at the mold wall in the direction normal to the mold wall, the first derivative of the pressure in this direction is set to zero, in accordance with the Darcy's law.
- (8) The temperature of the resin at the inlet is assumed to be equal to the room-temperature.
- (9) The temperature of the fiber preform and the resin in contact with the tool plate is set equal to the temperature of the tool plate. In other words, a zero resistance to the heat transfer from the tool plate to the preform and the resin is assumed.
- (10) The temperature at the top surface of the high-permeability medium is taken to be governed by a convective flux to the environment. Following the procedure described in our recent work [15], a heat transfer coefficient is assessed as  $h = 30$  W/m<sup>2</sup>/K, while the film temperature is set to  $T_{\text{film}} = 295$  K.
- (11) The thermal flux at the right hand side of the computational domain is set to zero.
- (12) The degree of polymerization of the resin at the inlet is set to an initial value which was determined using the procedure described in Section 3.

At the beginning of each new time step, the pressure, velocity, fill-fraction parameter, permeability, temperature and degree of polymerization fields are known. Specifically, at the beginning of a simulation run, the only control-volumes filled with resin are the ones associated with the inlet (the left hand side of the computational domain). From the known pressure ( $P_{\text{in}}$ ) at the centroid of these control-volumes and the known pressure ( $P_{\text{vac}}$ ) at the centroid of the surrounding control-volumes at the flow front, and using the known initial permeability, temperature and degree of polymerization fields and the Darcy's law, Eq. (4), the flow velocities at the flow front are calculated. These velocities are assumed to remain constant over a small time step. As discussed earlier, mold filling is treated as a quasi steady-state process in which the steady-state condition is assumed to hold over a small time step. To ensure stability of such an approach, the time increment associated with a given computational step is set equal to the minimum time needed to completely fill one of the previously partially filled control-volume at the flow front. In some cases, however, more than one flow-front control-volume becomes simultaneously filled within the selected time increment.

The velocities obtained above are next used to solve the energy conservation equation and to obtain the temperature field at the end of the time step. Next, the temperature is assumed to vary linearly over the time

step and the resulting degree of polymerization field computed. This was done in two steps: (a) First a change in the degree of polymerization due to the resin exposure to elevated temperatures over the given time step is calculated and the corresponding change in the viscosity of the resin within each control-volume calculated (details of the calculation are presented in the next section); (b) next, the change in the resin viscosity within all fully or partially filled cells due to the resin flow into and out of the control-volumes is calculated. The average temperature and the average degree of polymerization values for the given time increment are used to recalculate the pressure and velocity fields and to recalculate the minimal time increment needed to completely fill one of the previously unfilled control-volumes at the flow front. The resulting velocity fields are used to recalculate the temperature field. This procedure is repeated until a preset convergence limit is reached with respect to the minimal time increment for filling one flow-front control-volume.

Once the convergence is attained, mold-filling simulation is continued over the next time step. Toward that end, the pressures at the centroid of the filled control-volumes are declared as unknowns and the system of linear algebraic equations, Eq. (16), reassembled and solved.

The procedure described above is repeated until the entire computational domain is filled with the resin (if the objective of the simulation is to determine the filling time) or up to a certain time shorter than the filling time (if the objective of the simulation is the analysis of the flow-front shape).

### 3. Rheology of the NBV-800 epoxy VARTM resin

NBV-800 is a two-component, toughened, epoxy-based resin which is frequently used in VARTM applications. Due to its low room-temperature viscosity ( $\sim 300$  cps,  $1 \text{ cps} = 10^{-3} \text{ kg/m/s}$ ), NBV-800 is recommended for room-temperature preform infiltration. Upon infiltration, the following curing cycle is recommended: heating from the room-temperature to  $\sim 400$  K at a heating rate  $1.67 \text{ K min}^{-1}$  followed by holding at 400 K for 2 h.

The gelation temperature versus time curve for the NBV-800 is displayed in Fig. 5 [9]. To model the

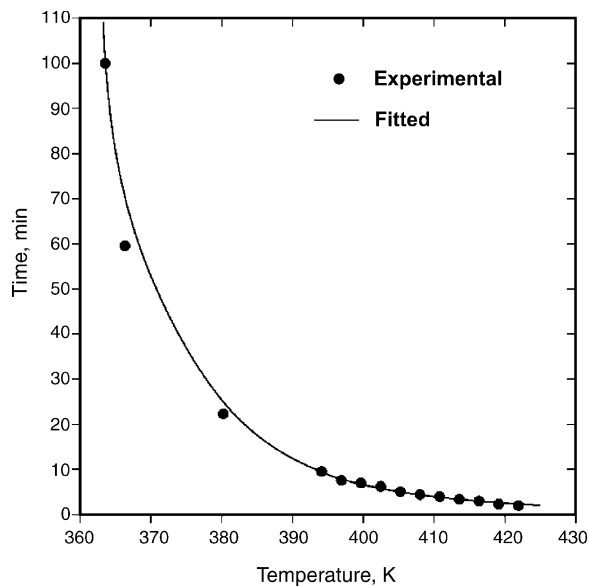


Fig. 5. Isothermal temperature–time gelation curve for NBV-800 epoxy resin.

kinetics of polymerization of this resin, it is assumed that, at each temperature, the onset of gelation corresponds to a same value of the degree of polymerization,  $p$ . The degree of polymerization at the onset of gelation was determined by requiring that after the recommended curing cycle given above, the NBV-800 is practically fully-polymerized ( $P = 0.999$ ). This procedure yielded  $P = 0.17$  at the onset on gelation. Assuming a first-order reaction kinetics for the isothermal polymerization process, the degree of polymerization is taken to evolve with time at a constant temperature as:

$$p = 1 - \exp^{-k(T)t} \quad (17)$$

where the temperature-dependent reaction rate constant  $k(T)$  is defined as:

$$k(T) = A \exp^{-Q/RT} \quad (18)$$

By setting  $P = 0.17$  and using the resin gelation data from Fig. 5, the two Arrhenius kinetic parameters are determined via least-squares fitting procedure as  $A = 89.61 \text{ min}^{-1}$ , and  $Q = 11,600 \text{ J/mol}$ . A comparison of the fitting function (the solid line) and the experimental data (solid circles) in Fig. 5 shows that

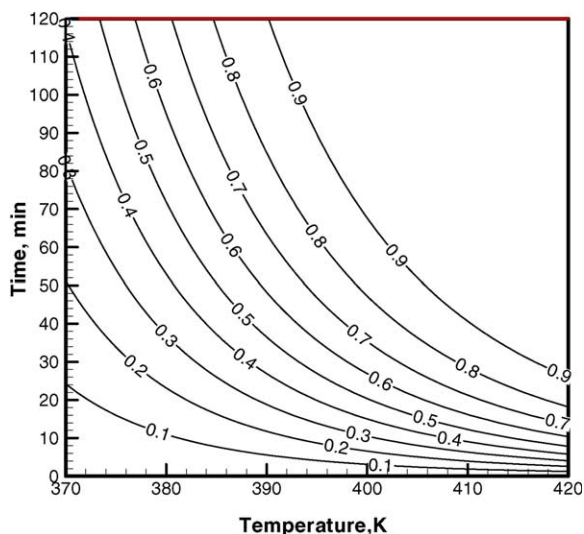


Fig. 6. Variation of the degree of polymerization in the NBV-800 epoxy resin with time during isothermal holdings at different temperatures.

the assumption regarding the first-order reaction kinetics for polymerization of the NBV-800 is justified. The variation of the degree of polymerization in the NBV-800 during holding time at various temperatures is shown in Fig. 6. It is seen that isothermal curing at 400 K gives rise to a practically complete polymerization of the NBV-800 which is consistent with the recommended holding stage of the curing cycle discussed above.

The evolution of the degree of polymerization of a material point in the resin subjected to a non-uniform temperature history during preform infiltration is obtained by integrating the following differential equation:

$$\frac{dp}{dt} = \frac{\partial p}{\partial t} + \frac{\partial p}{\partial T} \frac{\partial T}{\partial t} \tag{19}$$

to obtain:

$$p_{t+\Delta t} = (1 - (1 - p_t)\exp(-A \int_t^{t+\Delta t} \exp\left(-\frac{Q}{RT(t')}\right) dt') \tag{20}$$

where subscripts  $t$  and  $t + \Delta t$  are used to denote the value of a quantity at the beginning and at the

end of a time step with the duration  $\Delta t$  and the integral can be readily evaluated using numerical integration.

Next, following our recent work, the resin viscosity at each temperature is taken to be a single power-law function of the degree of polymerization [9] and that there is a degree of polymerization invariant thermal-thinning effect. Consequently, the resin viscosity is defined as:

$$\eta = [\eta_{p=0} + (\eta_{p=1} - \eta_{p=0})p^{11.3}] \cdot e^{-(Q^*/RT)((1/T)-(1/T_{RT}))} \tag{21}$$

where  $\eta_{p=0}$  (=300 cps) and  $\eta_{p=1}$  (=10,000 cps) are the room-temperature viscosity of fully un-polymerized and fully polymerized resin,  $Q^*$  (=2600 J/mol) [9] is a thermal-thinning activation energy and  $T_{RT}$  (=295 K) is the room-temperature. The effect of degree of polymerization and the temperature on the logarithm of viscosity of the NBV-800 is shown in Fig. 7. It is seen that the degree of polymerization has a substantially larger effect on viscosity of the NBV-800 than the temperature and that the effect of temperature on the relative change in viscosity of the NBV-800 is quite similar at different levels of the degree of polymerization.

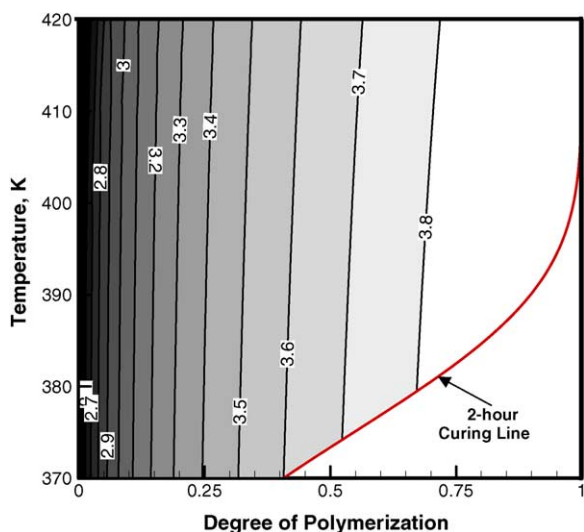


Fig. 7. Variation of the logarithm of viscosity in the NBV-800 epoxy resin with the degree of polymerization and temperature.

## 4. Results and discussion

### 4.1. Room-temperature mold filling simulations

The control-volume finite-element method developed in Sections 2.1–2.3 is utilized in this section to analyze preform infiltration with the NBV-800 epoxy resin at room-temperature. The details regarding the preform dimensions including the thicknesses of the high-permeability medium, the peel-ply and the fiber-preform as well as the values of the planar and the through-the-thickness permeabilities of these layers are given in Section 2.3 and in Table 1. The value for room-temperature viscosity of the neat NBV-800 resin is given in Table 1.

Since, no experimental investigation is carried out as part of this work, the present model is validated using the experimental flow visualization results of Lee and co-workers [7] for room-temperature infiltrations of a carbon preform with three different mineral oils: DOP oil (room-temperature viscosity 43 cps), Mobil Extra Heavy Oil (room-temperature viscosity 320 cps), Mobil BB oil (room-temperature viscosity 530 cps). Both the computed shapes of the flow front and the infiltration times (the results not shown for brevity) are found to agree quite well with their experimental counterparts.

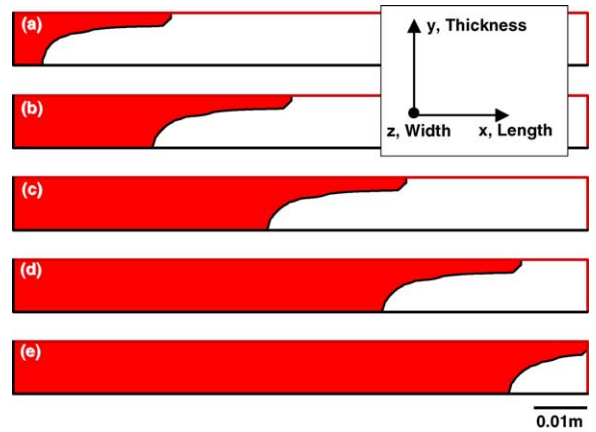


Fig. 8. Resin flow fronts during room-temperature infiltration at the filling times: (a) 5.2 s; (b) 42.9 s; (c) 111.8 s; (d) 211.7 s; and (e) 346.8 s.

for brevity) showed that the lag distance,  $l_1$ , reaches a nearly constant, steady-state value of  $\sim 27$  mm, approximately 4.4 s after the start of the mold filling process. This value of the lag distance is in a reasonably good agreement with the corresponding value (25 mm) obtained using the following analytically-derived equation proposed by Ni et al. [12]:

$$l_1 = h_{FP} \frac{\left(1 - \sqrt{\frac{K_z}{K_x} \frac{h_{HPM}}{h_{FP}}}\right) + \sqrt{\left(1 - \sqrt{\frac{K_y}{K_x} \frac{h_{HPM}}{h_{FP}}}\right)^2 + \pi \sqrt{\frac{K_y}{K_x} \frac{h_{HPM}}{h_{FP}}}}{\frac{\pi}{2} \sqrt{\frac{K_y}{K_x}}} \quad (22)$$

Fig. 8(a)–(e) show the NBV-resin flow-fronts at infiltration times of 5.2, 42.9, 111.8, 211.7 and 346.8 s, respectively. As expected, it is seen that in the preform length direction, the resin flows primarily through the high-permeability medium. Infiltration of the peel-ply and the fiber-preform, on the other hand, is primarily the result of resin flow from the fully-infiltrated high-permeability medium into the peel-ply and the fiber preform in the through-the-thickness direction. Consequently, the flow front in the fiber preform lags behind the flow front in the high-permeability medium. Short-time simulation results of the evolution of the resin flow front (not included here

where  $h_{FP}$  and  $h_{HPM}$  are the thicknesses of the fiber preform and the high-permeability medium, respectively and  $K_x$  and  $K_y$  are the fiber-preform in-plane and through-the-thickness permeabilities, respectively. When applying Eq. (22), the thickness of the peel ply is added to the thickness of the fiber preform,  $h_{FP}$ , and the permeabilities of the peel ply set equal to the ones of the fiber-preform. This simplification is fully justified based on the permeability data shown in Table 1.

The isothermal mold-filling simulation yielded a time of 471 s for a complete filling of the mold. This value, as well as the flow-front profiles displayed in

Fig. 8(a)–(e), are found not to be significantly affected when the mesh size is reduced by a factor of 2. Consequently, all the remaining calculations reported here were carried out using the mesh size reported in Section 2.3.

#### 4.2. Non-isothermal mold filling simulations

The control-volume finite-element method developed in Sections 2.1–2.3 is utilized in this section to analyze preform infiltration with the NBV-800 epoxy resin under different thermal histories of the tool plate. The details regarding the preform dimensions including the thicknesses of the high-permeability medium, the peel-ply and the fiber-preform as well as the values of the planar and the through-the-thickness permeabilities of these layers are given in Section 2.3 and in Table 1. The change of the viscosity of the NBV-800 resin with the degree of polymerization and with temperature is discussed in Section 3.

The mold-filling simulations carried out in this section involved ramping of the tool-plate temperature, from the onset of preform infiltration, at a constant heating rate of 0.03 K/s until a desired (holding) temperature is reached and holding the temperature constant thereafter until the completion of mold filling. The effect of the holding temperature on the time required to fill a half of the mold (the half-filling time) and the time for complete filling of the mold (the complete-filling time) are displayed in Fig. 9(a) and (b), respectively. It is seen that the minimum half-filling time is attained for the holding temperature of  $\sim 334$  K, while any heating of the tool plate increases the complete-filling time. This finding can be readily explained by considering the direct (thermal-thinning) effect of the temperature on the resin viscosity and its indirect effect via an increase in the degree of polymerization in the resin. The thermal-thinning effect is dominant at shorter infiltration times when the degree of polymerization in the resin is close to zero. Consequently, the resulting lower viscosity of the resin can give rise to a decrease in the infiltration time, Fig. 9(a). Contrary, at longer infiltration times, a viscosity increase due to the associated increase in the degree of polymerization of the resin becomes dominant and, consequently, the infiltration times are increased, Fig. 9(b).

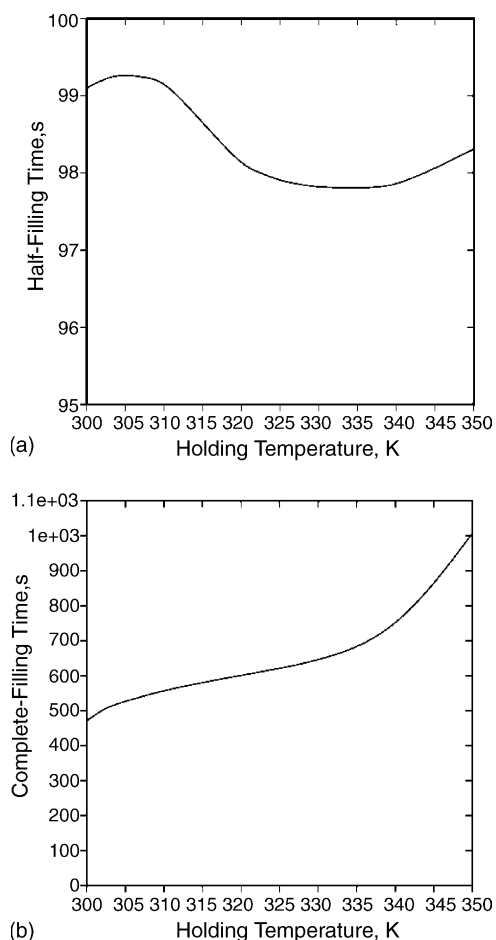


Fig. 9. The effect of the tool-plate holding temperature on: (a) the mold half-filling time and (b) the complete-filling time. The tool-plate heating rate from the room-temperature to the holding temperature is fixed at 0.3 K/s.

To demonstrate the effect of thermal-thinning at short infiltration times, the flow-front shape and the temperature and the viscosity contour plots at fill fraction of the mold of  $\sim 13\%$  for the case of the tool-plate heating from the onset of infiltration at a rate of 5 K/s are shown in Fig. 10(a)–(c), respectively. A comparison of the results displayed in Fig. 10(a) and Fig. 8(a)–(e) shows that, due to a lower viscosity of the resin in the vicinity of the tool-plate, there is a measurable contribution of the resin flow in the longitudinal direction which changes the shape of the flow front. Specifically, the largest lag distance in the preform is not at the tool-plate surface but somewhat removed from it. A comparison of the results displayed

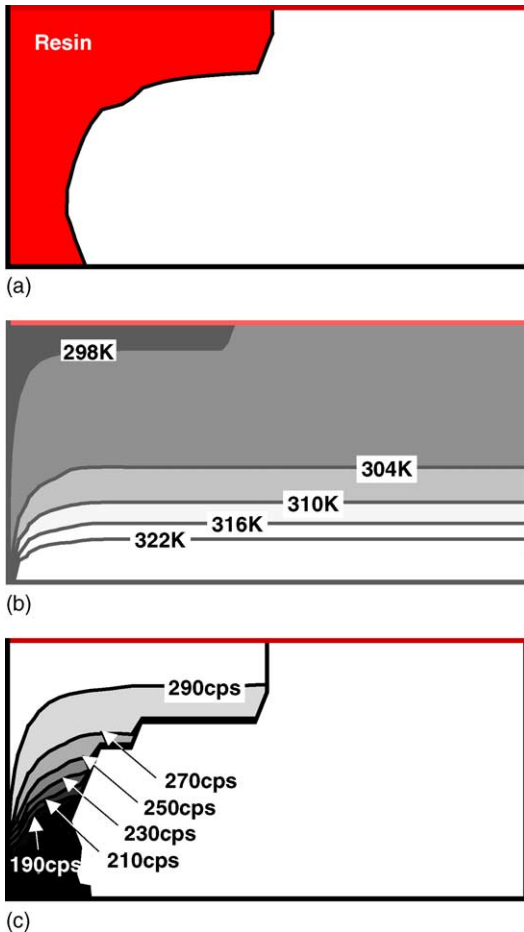


Fig. 10. (a) The flow front; (b) the temperature contour plot; and (c) the resin viscosity contour plot for the case of preform infiltration in which the tool plate is heated, from the onset of infiltration at a rate of 5 K/s for  $\sim 5$  s.

in Fig. 10(b) and (c) shows a direct correlation between the temperature and the resin viscosity at shorter infiltration times when the direct thermal-thinning effect of the temperature on resin viscosity is prevalent.

#### 4.3. Optimization of the mold filling process

The model developed in the present work enables determination of an optimum ramping/holding thermal history of the tool plate which can give rise to a minimum complete-filling time. An example of such an optimization procedure is presented in this section.

In general, optimization of the preform-infiltration process under non-isothermal conditions can be done

by decomposing the time–temperature profile of the tool plate into a number of constant heating-rate ramping steps and a number of constant-temperature holding steps. Then the ramping heating rates and holding temperatures and times can be used as optimization parameters. An optimization procedure, such as the simplex method [13] or the genetic algorithm [14], can then be used to determine the optimum thermal history of the tool plate which minimizes the complete-filling time. Such an optimum analysis will be used in our future work. In this paper, however, we report the results of a simple two-parameter optimization analysis which does not entail the use of an optimization algorithm.

Based on the results presented in the previous section, it was concluded that heating of the tool plate should start only after a substantial fraction of the mold has been infiltrated with the resin at the room-temperature. Otherwise, the associated prolonged heating of the resin during preform infiltration gives rise to an increase in the degree of polymerization and, in turn, to an increase in the resin viscosity causing the rate of infiltration to decrease. Toward that end, a two-parameter optimization analysis is carried out in which the fraction of the mold filled with the resin at the room-temperature and the heating rate at which the tool plate is subsequently heated are used as the optimization parameters. The first parameter is varied from 0.5 to 1.00 in increments of 0.1, while the second

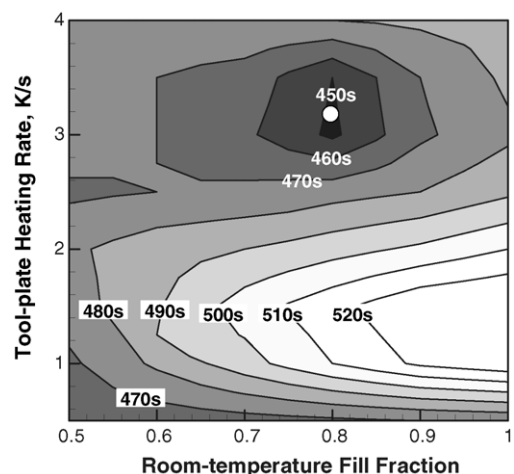


Fig. 11. Variation of the complete-filling time with the room-temperature fill fraction and the tool-plate heating rate. The solid white circle is used to denote the minimum complete-filling time.

parameter is varied from 0.5 to 4 K/s in increments of 0.25 K/s. The results of this optimization analysis are presented using a complete-filling time contour plot shown in Fig. 11. It is seen that relative to the case of complete mold-filling at the room-temperature,  $\sim 80\%$  preform infiltration at the room-temperature followed by heating of the tool plate at a rate of  $\sim 3.2$  K/s can reduce the complete-filling time by  $\sim 5\%$ , from 471 to 447 s. While this level of complete-filling time reduction does not appear very significant, one can generally expect more significant complete-filling time reductions in the VARTM preforms with more complex shapes. Unfortunately, three-dimensional modeling of the filling and heating stages of the VARTM process in preforms of a more realistic shape is beyond the scope of the present work.

## 5. Conclusions

Based on the results obtained in the present work, the following main conclusions can be drawn:

1. By adding to the incompressible-fluid mass conservation equation an energy conservation equation and an equation for the time and temperature evolution of the degree of polymerization of the resin, the control-volume finite-element method originally proposed by Lee and co-workers [4–8] has been extended to analyze preform infiltration stage of a high-permeability medium based vacuum-assisted resin transfer molding (VARTM) process.
2. Simulations of the preform infiltration process under non-isothermal conditions showed that, at short infiltration times, the effect of tool-plate heating can be beneficial and can lead to an increase in the rate of infiltration. This effect has been attributed to a thermal-thinning based reduction in the resin viscosity.
3. An optimization analysis of the VARTM preform infiltration process showed that, in order to take a full advantage of tool-plate heating,  $\sim 70\text{--}80\%$  of the mold should be filled with the resin at the room-temperature before heating of the tool-plate is initiated. For the simple rectangular geometry of the fiber preform used in the present work,  $\sim 80\%$  room-temperature preform infiltration followed by a tool-plate heating at a rate of  $\sim 3.2$  K/s, can reduce the

infiltration time by  $\sim 5\%$  relative to the room-temperature complete-infiltration time.

## Acknowledgements

The material presented in this paper is based on work supported by the U.S. Army Grant Number DAAD19-01-1-0661. The authors are indebted to Drs. Walter Roy, Fred Stanton, William DeRosset and Dennis Helfritch of ARL for the support and a continuing interest in the present work. The authors also acknowledge the support of the Office of High Performance Computing Facilities at Clemson University.

## Appendix A. Global to local systems transformation

While deriving the continuity equation for a single control-volume, Eq. (8), a local ( $x$ - $y$ - $z$ ) coordinate system is used in the present two-dimensional formulation. In this coordinate system, the  $z$ -axis is aligned with the preform-surface normal. Furthermore since the  $z$ -coordinate is not explicitly considered (and can be set to zero), due to a two-dimensional nature of the formulation. Also, when the fiber preform is planar, the local coordinate system for each cell is taken to coincide with the global  $X$ - $Y$ - $Z$  coordinate system. When a finite-element mesh is generated, the nodal coordinates are defined with respect to the global coordinate system. Since, Eq. (8) is defined with respect to a local coordinate system of the control-volume in question, the nodal coordinates must be transformed from the global to the local coordinate system before Eq. (8) can be used. To transform the global ( $X, Y, Z$ ) coordinates into the corresponding local ( $x, y, z$ ) coordinates of a node the following matrix equation should be used:

$$\begin{bmatrix} x \\ y \\ z \end{bmatrix} = \begin{bmatrix} \frac{n_x^2 n_z + n_y^2}{n_x^2 + n} & \frac{n_x^2 n_z + n_y^2}{n_x^2 + n} & -n_x \\ \frac{n_x n_y (n_z - 1)}{n_x^2 + n_y^2} & \frac{n_x n_y (n_z - 1)}{n_x^2 + n_y^2} & -n_y \\ n_x & n_x & n_x \end{bmatrix} \begin{bmatrix} X \\ Y \\ Z \end{bmatrix} \quad (\text{A.1})$$

where  $n_x$ ,  $n_y$  and  $n_z$  are the components of the element surface normal vector expressed in the global coordinate system.

The use of the local coordinate system is very important in handling the effect of the fiber orientation in the preform and the resultant anisotropy in preform permeability. In such cases, the fiber orientation in the preform surface is used to define one of the local ( $x$  or  $y$ ) axes.

## References

- [1] S.M. Lewit, J.C. Jakubowski, Low cost VARTM process for commercial and military applications, in: SAMPE International Symposium, 1997, pp. , p. 1173.
- [2] L.B. Nquyen, T. Juska, S.J. Mayes, Evaluation of low cost manufacturing technologies for large scale composite ship structures, in: AIAA/ASME/ASCE/AHS/ASC Structures, Structural Dynamics and Materials Conference, 1997, pp. , p. 992.
- [3] P. Lazarus, Resin infusion of marine composites, in: SAMPE International Symposium, 1996, pp. , p. 1447.
- [4] W.B. Young, K. Han, L.H. Fong, L.J. Lee, M.J. Liou, Flow simulation in molds with preplaced fiber mats, *Polym. Comp.* 12 (1991) 391.
- [5] W.B. Young, K. Rupel, K. Han, L.J. Lee, M.J. Liou, Analysis of resin injection molding in molds with preplaced fiber mats. I: Permeability and compressibility measurements, *Polym. Comp.* 12 (1991) 30.
- [6] W.B. Young, K. Rupel, K. Han, L.J. Lee, M.J. Liou, Analysis of resin injection molding in molds with preplaced fiber mats. II: Numerical simulation and experiments of mold filling, *Polym. Comp.* 12 (1991) 20.
- [7] X.D. Sun, S. Li, L.J. Lee, Mold filling analysis in vacuum-assisted resin transfer molding, part I: SCRIMP based on a high-permeable medium, *Polym. Comp.* 19 (1998) 807.
- [8] X.D. Sun, S. Li, L.J. Lee, Mold filling analysis in vacuum-assisted resin transfer molding, part II: SCRIMP based on grooves, *Polym. Comp.* 19 (1998) 818.
- [9] M. Grujicic, K.M. Chittajallu, Kinetics of polymerization of NBV-800 two-component epoxy-based resin, *J. Mater. Sci.*, submitted for publication.
- [10] K.H. Huebner, D.L. Dewhirst, D.E. Smith, T.G. Byrom, *The Finite Element Method For Engineers*, 4th ed. Wiley–Interscience, 2001.
- [11] R.J. Johnson, R. Pitchumani, Enhancement of flow in VARTM using localized induction heating, *Comp. Sci. Technol.* 63 (2003) 2201.
- [12] J. Ni, Y. Zhao, L.J. Lee, S. Nakamura, Analysis of two-regional flow in liquid composite molding, *Polym. Comp.* 18 (1997) 254.
- [13] M. Grujicic, Y. Hu, G.M. Fadel, Optimization of the LENS<sup>TM</sup> rapid fabrication process for in-flight melting of the feed powder, *J. Mater. Synth. Process.* 9 (2002) 223.
- [14] M. Grujicic, G. Cao, B. Gersten, Optimization of the chemical vapor deposition process for carbon nanotubes fabrication, *Appl. Surf. Sci.* 191 (2002) 223.
- [15] M. Grujicic, K.M. Chittajallu, S. Walsh, Optimization of the VARTM process for enhancement of the degree of devolatilization of polymerization by-products and solvents, *J. Mater. Sci.* 38 (2003) 1729.